

Three-Dimensional ^{13}C -Detected CH_3 -TOCSY Using Selectively Protonated Proteins: Facile Methyl Resonance Assignment and Protein Structure Determination

John B. Jordan,[†] Helena Kovacs,[‡] Yuefeng Wang,[†] Mehdi Mobli,[§] Rensheng Luo,^{†,¶} Clemens Anklin,[#] Jeffrey C. Hoch,[§] and Richard W. Kriwacki^{*,†,£}

Contribution from the Department of Structural Biology, St. Jude Children's Research Hospital, Memphis, Tennessee 38105, Bruker Biospin AG, Fällanden, Switzerland, Department of Molecular, Microbial, and Structural Biology, University of Connecticut Health Center, Farmington, Connecticut 06030, Bruker Biospin Corporation, Billerica, Massachusetts 01821, and Department of Molecular Sciences, University of Tennessee Health Sciences Center, Memphis, Tennessee 38163

Received December 19, 2005; E-mail: richard.kriwacki@stjude.org

Abstract: Recent advances in instrumentation and isotope labeling methodology allow proteins up to 100 kDa in size to be studied in detail using NMR spectroscopy. Using $^2\text{H}/^{13}\text{C}/^{15}\text{N}$ enrichment and selective methyl protonation, we show that newly developed ^{13}C direct detection methods can be used to rapidly yield proton and carbon resonance assignments for the methyl groups of Val, Leu, and Ile residues. We present a highly sensitive ^{13}C -detected CH_3 -TOCSY experiment that, in combination with standard ^1H -detected backbone experiments, allows the full assignment of side chain resonances in methyl-protonated residues. Selective methyl protonation, originally developed by Kay and co-workers (Rosen, M. K.; Gardner, K. H.; Willis, R. C.; Parris, W. E.; Pawson, T.; Kay, L. E. *J. Mol. Biol.* **1996**, *263*, 627–636; Gardner, K. G.; Kay, L. E. *Annu. Rev. Biophys. Biomol. Struct.* **1998**, *27*, 357–406; Goto, N. K.; Kay, L. E. *Curr. Opin. Struct. Biol.* **2000**, *10*, 585–592), improves the nuclear relaxation behavior of larger proteins compared to their fully protonated counterparts, allows significant simplification of spectra, and facilitates NOE assignments. Here, we demonstrate the usefulness of the ^{13}C -detected CH_3 -TOCSY experiment through studies of (i) a medium-sized protein (CbpA-R1; 14 kDa) with a repetitive primary sequence that yields highly degenerate NMR spectra, and (ii) a larger, bimolecular protein complex (p21-KID/Cdk2; 45 kDa) at low concentration in a high ionic strength solution. Through the analysis of NOEs involving amide and Ile, Leu, and Val methyl protons, we determined the global fold of CbpA-R1, a bacterial protein that mediates the pathogenic effects of *Streptococcus pneumoniae*, demonstrating that this approach can significantly reduce the time required to determine protein structures by NMR.

Introduction

Solution NMR spectroscopy has emerged as a preeminent tool in studies of protein structure,⁴ dynamics,⁴ and intermolecular interactions.⁵ A key limitation, however, has been the size of molecules that can be studied. Recent advances in isotope labeling,² the development of TROSY-based methods,⁶

and the advent of cryogenic probes⁷ have extended the size limit associated with biomolecular NMR. In particular, perdeuteration has been shown to mitigate rapid heteronuclear (e.g., ^{13}C and ^{15}N) relaxation.⁸ However, this isotope labeling method drastically reduces the number of ^1H – ^1H NOEs that can be measured and subsequently used for protein structure determination. To allow the measurement of structurally informative NOEs in perdeuterated proteins, Kay and co-workers developed biosynthetic methods to selectively protonate methyl groups of Val, Ile, and Leu residues.^{1–3,9} These residues are abundant (~21% of all residues)^{10,11} and are often found within the hydrophobic cores of globular proteins. In addition, the protons of methyl groups in these residues can be detected with high sensitivity.⁹

[†] St. Jude Children's Research Hospital.

[‡] Bruker Biospin AG.

[§] University of Connecticut Health Center.

[¶] Current address: Department of Chemistry and Biochemistry, University of Missouri—St. Louis, St. Louis, MO.

[#] Bruker Biospin Corporation.

[£] University of Tennessee Health Sciences Center.

(1) Rosen, M. K.; Gardner, K. H.; Willis, R. C.; Parris, W. E.; Pawson, T.; Kay, L. E. *J. Mol. Biol.* **1996**, *263*, 627–636.

(2) Gardner, K. G.; Kay, L. E. *Annu. Rev. Biophys. Biomol. Struct.* **1998**, *27*, 357–406.

(3) Goto, N. K.; Kay, L. E. *Curr. Opin. Struct. Biol.* **2000**, *10*, 585–592.

(4) Kay, L. E. *J. Magn. Reson.* **2005**, *173*, 193–207.

(5) Lian, L. Y.; Barsukov, I. L.; Sutcliffe, M. J.; Sze, K. H.; Roberts, G. C. *Methods Enzymol.* **1994**, *239*, 657–700.

(6) Pervushin, K.; Riek, R.; Wider, G.; Wuthrich, K. *Proc. Natl. Acad. Sci. U.S.A.* **1997**, *94*, 12366–12371.

(7) Kovacs, H.; Moskau, D.; Spraul, M. *Prog. NMR Spectrosc.* **2005**, *46*, 131–155.

(8) Venter, R. A.; Huang, C. C.; Farmer, B. T., II; Trolard, R.; Spicer, L. D.; Fierke, C. A. *J. Biomol. NMR* **1995**, *5*, 339–344.

(9) Kay, L. E.; Gardner, K. H. *Curr. Opin. Struct. Biol.* **1997**, *7*, 722–731.

(10) Tugarinov, V.; Choy, W. Y.; Orekhov, V. Y.; Kay, L. E. *Proc. Natl. Acad. Sci. U.S.A.* **2005**, *102*, 622–627; Epub 2005 Jan 06.

(11) Tugarinov, V.; Kay, L. E. *Chembiochem* **2005**, *6*, 1567–1577.

These factors facilitate the assignment and measurement of numerous long-range amide–methyl and methyl–methyl NOEs,^{1,3,12} which allow protein global folds to be determined. Notably, this method was demonstrated by Tugarinov et al., through near complete assignment of Ile, Leu, and Val methyl resonances¹³ and global fold determination of the 723-residue enzyme, malate synthase G (MSG).¹⁰

The use of methyl-protonated, ²H/¹³C/¹⁵N-labeled proteins for structure determination requires sequence-specific assignment of methyl ¹H (¹H_{Me}) and ¹³C (¹³C_{Me}) resonances. These assignments can be established through correlations of methyl resonances with those assigned previously using standard backbone assignment procedures (e.g., ¹H_N/¹⁵N, ¹³C_α/¹³C_β, and ¹³C_γ).¹³ We focus here on methods involving correlations of ¹H_{Me}/¹³C_{Me} resonances with ¹³C_{α,β,γ} resonances. Kay et al. demonstrated an “out-and-back” ¹H methyl-detected experiment that correlated ¹H_{Me}/¹³C_{Me} chemical shifts with ¹³C_{α,β,γ} chemical shifts of Ile and Leu residues and ¹³C_{α,β} chemical shifts of Val residues.¹³ The utility of this experiment was demonstrated with 0.9 mM methyl-protonated ²H/¹³C/¹⁵N-labeled MSG for which a 3D spectrum was acquired in 59 h at 800 MHz using a conventional probe. Between 60 and 86% of ¹H_{Me}/¹³C_{Me} and ¹³C_{α,β,γ} correlations were established through analysis of this spectrum. An alternative approach based on ¹³C detection, termed HCC-TOCSY, allowed similar correlations to be observed¹⁴ in proteins produced using fractional deuteration.

In the past, direct detection of ¹³C resonances for biopolymers was impractical due to low signal-to-noise ratios (S/N). However, isotopic enrichment of proteins with ¹³C and the availability of highly sensitive, cryogenic probes have spawned a generation of new protein NMR methods based on ¹³C detection.⁷ The HCC-TOCSY experiment was first demonstrated by Hu and co-workers¹⁴ using either partially deuterated or fully protonated protein samples (0.8 mM, 48 kDa FkpA, 90% ²H, uniformly ¹³C/¹⁵N-labeled or 1 mM 16 kDa Ccm-E, uniformly ¹³C/¹⁵N-labeled) using 500 or 600 MHz dual-channel (¹H/¹³C) cryogenic probes optimized for ¹³C detection. Spectra for FkpA and Ccm-E were acquired in 117 h each. We present here a three-dimensional ¹³C-detected experiment termed CH₃-TOCSY, which allows full assignment of ¹H_{Me} and ¹³C_{Me} resonances in two [I, L, V] methyl-protonated ²H/¹³C/¹⁵N-labeled proteins. This experiment is specifically designed for proteins labeled in this manner, and making use of the abundant methyl ¹H magnetization allows the correlation of ¹H_{Me} (*t*₁) and ¹³C_{Me} (*t*₂) chemical shifts with other side chain ¹³C chemical shifts using homonuclear isotropic mixing of ¹³C nuclei. This approach is distinctly different from previous methods in that it allows complete assignment of “nonlinearized”,¹³ methyl-protonated residues in an otherwise fully deuterated background using ¹³C detection. We demonstrate the performance of this experiment in studies of a small protein (CbpA-R1; 14 kDa) and a labeled protein (p21-KID; 10 kDa) within a 45 kDa binary complex (p21-KID/Cdk2). Further, we demonstrate how information gained from the 3D CH₃-TOCSY experiment can be applied for streamlined determination of the CbpA-R1 structure using a limited number of methyl–methyl (¹H_{Me}–¹H_{Me}), methyl–HN (¹H_{Me}–¹H_N), and HN–HN (¹H_N–¹H_N) NOEs.

Choline binding protein A (CbpA) is the major surface adhesin of *Streptococcus pneumoniae* (pneumococcus), the most common bacterial pathogen of children.¹⁵ CbpA consists of five domains, two of which (CbpA-R1 and -R2) act as adhesion domains through interactions with polymeric immunoglobulin receptor (pIgR) on the surface of epithelia in the human nasopharynx.^{16–20} CbpA-R1 and -R2 (~120 amino acids each) bind directly to the extracellular domain of pIgR^{16,21,22} and mediate invasion of intact pneumococci into the human blood stream. Because CbpA-R1 and -R2 play unique roles in pneumococcal pathogenesis,²² small-molecule inhibitors or vaccines directed against them may be therapeutically beneficial. In support of such efforts, we used traditional, triple-resonance NMR methods to determine the structure of CbpA-R2²¹ and report here the application of selective [I, L, V] methyl protonation and the ¹³C-detected CH₃-TOCSY method, in addition to a limited number of conventional NMR methods, to determine the structure of CbpA-R1. CbpA-R1 and -R2 consist of extensively helical and highly repetitive sequences (12 leucine zipper repeats) that result in highly degenerate NMR spectra; therefore, the spectral editing associated with selective methyl protonation served to simplify NMR analysis of CbpA-R1. We have critically evaluated our structural results for two closely related domains obtained using the traditional (CbpA-R2) and newer, streamlined (CbpA-R1) approach.

We recently reported partial backbone and ¹³C_β resonance assignments for the kinase inhibitory domain (KID) of the human cell cycle regulatory protein, p21^{Waf1/Cip1} (p21-KID), bound to Cdk2, cyclin A, and Cdk2/cyclin A.²³ In an effort to gain insights into the structure of p21-KID bound to Cdk2, we prepared [I, L, V]-protonated, ²H/¹³C/¹⁵N-labeled p21-KID, formed the binary complex with unlabeled Cdk2, and used the ¹³C-detected CH₃-TOCSY experiment to assign all of the selectively protonated CH₃ resonances of p21-KID. These results demonstrate the feasibility of this ¹³C detection method to studies of protein assemblies of “modest” size (45 kDa) under challenging conditions, including relatively low protein concentration (0.3 mM) and relatively high ionic strength (20 mM phosphate buffer in the presence of 50 mM arginine).

Materials and Methods

Preparation of NMR Samples. Unlabeled, human Cdk2²⁴ and isotope-labeled CbpA-R1²¹ and p21-KID²³ were expressed in *E. coli* and purified using established procedures. ²H/¹³C/¹⁵N-labeled CbpA-R1 was prepared by culturing BL21(DE3) cells in isotope-labeled MOPS-based minimal media²⁵ using 1 g/L of ¹⁵N ammonium chloride and 2 g/L of ¹³C glucose in ²H₂O. ²H/¹³C/¹⁵N-labeled p21-KID was

(12) Metzler, W. J.; Leiting, B.; Pryor, K.; Mueller, L.; Farmer, B. T., II. *Biochemistry* **1996**, *35*, 6201–6211.

(13) Tugarinov, V.; Kay, L. E. *J. Am. Chem. Soc.* **2003**, *125*, 13868–13878.

(14) Hu, K.; Vogeli, B.; Pervushin, K. *J. Magn. Reson.* **2005**, *174*, 200–208.

(15) CDC Active Bacterial Core Surveillance Report (ABCS), *Streptococcus pneumoniae*; 2001.

(16) Zhang, J. R.; Mostov, K. E.; Lamm, M. E.; Nanno, M.; Shimida, S.; Ohwaki, M.; Tuomanen, E. *Cell* **2000**, *102*, 827–837.

(17) Gosink, K. K.; Mann, E. R.; Guglielmo, C.; Tuomanen, E. I.; Masure, H. R. *Infect. Immun.* **2000**, *68*, 5690–5695.

(18) Elm, C.; Braathen, R.; Bergmann, S.; Frank, R.; Vaerman, J. P.; Kaetzel, C. S.; Chhatwal, G. S.; Johansen, F. E.; Hammerschmidt, S. *J. Biol. Chem.* **2004**, *279*, 6296–6304; Epub 2003 Dec 3.

(19) Lu, L.; Lamm, M. E.; Li, H.; Corthesy, B.; Zhang, J. R. *J. Biol. Chem.* **2003**, *278*, 48178–48187; Epub 2003 Sep 17.

(20) Rosenow, C.; Ryan, P.; Weiser, J. N.; Johnson, S.; Fontan, P.; Ortqvist, A.; Masure, H. R. *Mol. Microbiol.* **1997**, *25*, 819–829.

(21) Luo, R.; et al. *EMBO J.* **2005**, *24*, 34–43; Epub 2004 Dec 16.

(22) Hammerschmidt, S.; Talay, S. R.; Brandtzaeg, P.; Chhatwal, G. S. *Mol. Microbiol.* **1997**, *25*, 1113–1124.

(23) Wang, Y.; Filippov, I.; Richter, C.; Luo, R.; Kriwacki, R. W. *ChemBiochem* **2005**, *6*, 2242–2246.

(24) Lacy, E. R.; Filippov, I.; Lewis, W. S.; Otieno, S.; Xiao, L.; Weiss, S.; Hengst, L.; Kriwacki, R. W. *Nat. Struct. Mol. Biol.* **2004**, *11*, 358–364.

prepared using similar methods with 1 g/L of ¹⁵N ammonium chloride, 4 g/L of ¹³C acetate, and ²H₂O. Selectively [I, L, V]-protonated, ²H/¹³C/¹⁵N-labeled CbpA-R1 and p21-KID were prepared through addition, 1 h prior to induction with isopropyl-β-D-thiogalactopyranoside (IPTG), of 60 mg/L of (¹³C₄, 99%, 3,3-D₂, 98%) 2-ketobutyric acid and 100 mg/L of (¹³C₅, 99%, 3-D₁, 98%) 2-keto-3-methylbutyric acid (Cambridge Isotope Laboratories, Andover, MA) to the individual cultures.²⁶ Cells were grown for an additional 4 h at 37 °C and harvested by centrifugation. Isotope-labeled, His-tagged forms of CbpA-R1²¹ and p21-KID²³ were purified as previously described. NMR samples of CbpA-R1 (1 mM) were prepared using 10 mM potassium phosphate, pH 6.5, 50 mM NaCl, 10% ²H₂O (v/v), and 0.02% sodium azide (w/v). Samples of p21/Cdk2 (0.3 mM) were prepared using 20 mM potassium phosphate, pH 6.5, 50 mM arginine, 8% ²H₂O (v/v), 5 mM DTT, and 0.02% sodium azide (w/v) (p21-KID NMR buffer). The p21/Cdk2 complex was isolated using size exclusion chromatography (Superdex 200, Amersham-Pharmacia) in HEPES buffer²³ followed by exchange into p21-KID NMR buffer using ultrafiltration (Centricon units, Amicon).

NMR Experiments. Two NMR spectrometers were used: a Bruker AVANCE 800 equipped with a ¹H and ¹³C detect, triple-resonance cryogenic probe and a Varian INOVA 600 equipped with a room temperature triple-resonance gradient probe. All spectra were recorded at a sample temperature of 298 K and were processed with NMRPipe²⁷ using cosine apodization and zero-filling prior to Fourier transformation in the direct dimensions. Indirect dimensions were doubled using forward-backward linear prediction (mirror-image for CT experiments) followed by cosine apodization and zero-filling prior to Fourier transformation. In all ¹H-detected experiments recorded at 800 MHz, the direct dimension was acquired using a spectral width of 14 368 Hz with 1k complex points. Gradient- and sensitivity-enhanced 2D ¹H-¹⁵N TROSY spectra^{28–30} for CbpA-R1 were recorded at 800 MHz using a 2433 Hz spectral width with 128 complex points in the indirect ¹⁵N (*F*₁) dimension. Backbone resonance assignments were determined through the analysis of data from two experiments, 3D CT-HNCACB³¹ and CT-HN(CO)CACB³¹ recorded at 800 MHz with the following spectral parameters in their indirect dimensions: ¹⁵N (*F*₂) spectral width, 2433 Hz with 46 complex points, ¹³C (*F*₁) spectral width, 12 876 Hz with 156 complex points. The transformed data sets were reduced in the direct dimension to include only the regions of interest. In addition, the program MARS³² was used to assist in making backbone assignments for CbpA-R1. These assignments were then confirmed through the analysis of a 4D ¹H_N-¹H_N NOESY spectrum³³ acquired at 600 MHz using the following spectra parameters: ¹H (*F*₄) spectral width, 6982 Hz with 1k complex points; ¹⁵N (*F*₂/*F*₃) spectral widths, 1900 Hz with 23 complex points, HN spectral width, 1600 Hz with 18 complex points (*F*₁). ¹⁵N and ¹³C NOESY-HSQC spectra were acquired at 800 MHz to obtain distance restraints using mixing times of 100 and 160 ms. Acquisition of these spectra was tailored to methyl-protonated, ²H/¹³C/¹⁵N-labeled CbpA-R1 as follows. A reduced spectral width was used for the indirect proton dimensions (4400 Hz), which led to folding of ¹H_M resonances to a position downfield of ¹H_N resonances. Further, a reduced spectral width was used in the ¹³C indirect dimension of the 3D ¹³C NOESY-HSQC spectrum. The spectral parameters were as follows: For 3D ¹⁵N-edited NOESY-HSQC, ¹H (*F*₃) spectral width,

14 368 Hz with 1k complex points; ¹⁵N spectral width (*F*₂), 2433 Hz with 38 complex points; ¹H (*F*₁) spectral width, 4400 Hz with 90 complex points. For 3D ¹³C-edited NOESY-HSQC, ¹H (*F*₃) spectral width, 14 368 Hz with 1k complex points; ¹³C spectral width (*F*₂), 4426 Hz with 64 complex points; ¹H (*F*₁) spectral width, 8000 Hz with 124 complex points. Last, the 3D CNH-NOESY experiment was recorded at 800 MHz using the following acquisition parameters: ¹H (*F*₃) spectral width, 14 368 Hz with 1k complex points; ¹⁵N spectral width (*F*₂), 2433 Hz with 40 complex points; ¹H (*F*₁) spectral width, 2414 Hz with 50 complex points. ¹H-detected spectra using p21/Cdk2 were acquired and backbone assignments made as described in Wang et al.²³

A 3D ¹³C-detected CH₃-TOCSY spectrum was recorded for selectively [I, L, V]-protonated, ²H/¹³C/¹⁵N-labeled CbpA-R1 at 800 MHz using 8 scans per increment. The ¹³C spectral width was 14 124 Hz with 1k complex points in the direct ¹³C (*F*₃) dimension, and the spectral widths in the indirect ¹³C (*F*₂) and ¹H (*F*₁) indirect dimensions were 4828 Hz with 48 complex points and 960 Hz with 24 complex points, respectively. The same type of spectrum was recorded for selectively [I, L, V]-protonated, ²H/¹³C/¹⁵N-labeled p21-KID/unlabeled Cdk2 complex using 32 scans and the following spectral parameters: 14 124 Hz with 2k complex points in the direct ¹³C (*F*₃) dimension, and 3621 Hz with 38 complex points and 1280 Hz with 23 complex points in the indirect ¹³C (*F*₂) and ¹H (*F*₁) indirect dimensions, respectively. These spectra were processed in two ways. The first method made use of forward-backward linear prediction of the indirect dimensions, cosine apodization, and zero-filling followed by Fourier transformation using NMRPipe.²⁷ This led to the observation of one-bond ¹³C-¹³C couplings (¹*J*_{CC}) in the directly detected ¹³C dimension, which reduces spectral resolution and intensity. The second processing method made use of maximum entropy reconstruction of the direct (*F*₃) and indirect (*F*₂) ¹³C dimensions using Rowland NMR Tool Kit.³⁴ Deconvolution of the ¹³C-¹³C coupling constant (~35 Hz) was performed in the directly detected dimension to simplify multiplet patterns, eliminating one level of ¹³C-¹³C coupling (i.e., doublets were deconvoluted into singlets, triplets to doublets, etc.). The indirect ¹H dimension of this experiment (¹H_M) was processed by forward-backward linear prediction followed by cosine apodization and zero-filling prior to Fourier transform. Assignments for all resonances were made by the methods described herein using Felix software (Accelrys, Inc.). Resonance assignments for CbpA-R1 are provided in Supporting Information Table 1. The direct ¹H dimensions of spectra were referenced to external TSP, and the ¹³C and ¹⁵N indirect dimensions were referenced indirectly using the appropriate gyromagnetic ratios.³⁵ The directly detected ¹³C spectra were referenced indirectly with respect to the ¹H frequency of TSP.

Structure Calculation, Refinement, and Analysis. CbpA-R1 structures were calculated from an extended starting structure using the torsion angle dynamics (TAD) protocol of CNS³⁶ within ARIA 1.2,³⁷ and ¹H-¹H distances were derived from the analysis of 3D ¹⁵N and ¹³C NOESY-HSQC spectra. The program TALOS³⁸ was used to establish standardized psi (*ψ*) and phi (*Φ*) dihedral angle restraints for the three helices (*ψ* = -60° ± 10°; *Φ* = -40° ± 10°). Hydrogen bond restraints were utilized for amide moieties that exhibited slow exchange with ²H₂O. The final calculations generated 200 structures; the 20 with lowest energy were refined using the SANDER module of AMBER 8.0.³⁹ Solvent was represented by the generalized-Born (GB) model.⁴⁰ Structures were first energy minimized for 1 ps without restraints followed by 40 ps of simulated annealing from 400 to 0 K

(25) Neidhardt, F. C.; Bloch, P. L.; Smith, D. F. *J. Bacteriol.* **1974**, *119*, 736–747.

(26) Studier, F. W.; Rosenberg, A. H.; Dunn, J. J.; Dubendorff, J. W. *Methods Enzymol.* **1989**, *185*, 60–89.

(27) Delaglio, F.; Grzesiek, S.; Vuister, G. W.; Zhu, G.; Pfeifer, J.; Bax, A. *J. Biomol. NMR* **1995**, *6*, 277–293.

(28) Weigelt, J. *J. Am. Chem. Soc.* **1998**, *120*, 10778–10779.

(29) Loria, J. P.; Rance, M.; Palmer, A. G. R. *J. Magn. Reson.* **1999**, *141*, 180–184.

(30) Zhu, G.; Kong, X.; Sze, K. *J. Biomol. NMR* **1999**, *13*, 77–81.

(31) Yamazaki, T.; Lee, W.; Arrowsmith, C. H.; Muhandiram, D. R.; Kay, L. E. *J. Am. Chem. Soc.* **1994**, *116*, 11655–11666.

(32) Jung, Y. S.; Zweckstetter, M. *J. Biomol. NMR* **2004**, *30*, 11–23.

(33) Bax, A.; Clore, G. M.; Driscoll, P. C.; Gronenborn, A. M.; Ikura, M.; Kay, L. E. *J. Magn. Reson.* **1990**, *87*, 620–627.

(34) Stern, A. S.; Li, K. B.; Hoch, J. C. *J. Am. Chem. Soc.* **2002**, *124*, 1982–1993.

(35) Cavanagh, J.; Fairbrother, W. J.; Palmer, A. G., III; Skelton, N. J. *Protein NMR Spectroscopy*; Academic Press: New York, 1996.

(36) Stein, E. G.; Rice, L. M.; Brünger, A. T. *J. Magn. Reson., Ser. B* **1997**, *124*, 154–164.

(37) Ling, J. P.; Habeck, M.; Rieping, W.; Nilges, M. *Bioinformatics* **2003**, *19*, 315–316.

(38) Cornilescu, G.; Delaglio, F.; Bax, A. *J. Biomol. NMR* **1999**, *13*, 289–302.

(39) Case, D. A.; et al. *AMBER* **8**, 2004.

(40) Xia, B.; Tsui, V.; Case, D. A.; Dyson, H. J.; Wright, P. E. *J. Biomol. NMR* **2002**, *22*, 317–331.

Table 1. Statistics of 10 Lowest-Energy Structures of CbpA-R1 Based on Solution NMR Data

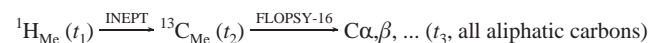
<i>total number of NOEs</i>	347
HN–HN NOEs (long range)	210 (6)
HN–methyl NOEs (long range)	126 (44)
methyl–methyl NOEs (long range)	11 (6)
<i>total hydrogen bond restraints</i>	57
<i>total dihedral restraints</i>	162
<i>distance restraint violations (avg. number per structure)^a</i>	
restraints violated by >0.50 Å	0.51
restraints violated by >0.30 Å	0.71
<i>torsion angle restraint violations (avg. number per structure)^a</i>	
ψ restraints violated by >5°	0
ϕ restraints violated by >5°	0
<i>average pairwise RMSD, Å^b</i>	
helix 1 (5–26)	1.82 ± 0.55
turn 1 (26–44)	2.94 ± 0.74
helix 2 (44–62)	1.13 ± 0.39
turn 2 (62–72)	2.48 ± 0.38
helix 3 (72–96)	1.65 ± 0.61
C-terminus (96–119)	4.64 ± 0.93
<i>average backbone RMSD to 1W9R²¹^b</i>	
helix 1 (5–26)	2.15 ± 0.46
turn 1 (26–44)	3.51 ± 0.55
helix 2 (44–62)	0.87 ± 0.11
turn 2 (62–72)	2.08 ± 0.40
helix 3 (72–96)	0.96 ± 0.15
C-terminus (96–119)	7.36 ± 0.65
<i>Ramachandran statistics^c</i>	
most favored region, %	77.5
allowed region, %	17.1
generously allowed region, %	4.5
disallowed region, %	0.9

^a Structures were calculated using ARIA1.2.³⁷ ^b Structural alignments and RMSD values were calculated using MolMol.⁴¹ ^c Ramachandran statistics determined using PROCHECK.⁴²

with all restraints. The distance and angle restraint force constants were 20 and 2 kcal mol⁻¹Å⁻², respectively. The average of these 20 structures was compared with the previously determined structure for CbpA-R2,²¹ which exhibits 78% sequence identity to CbpA-R1. Alignments and statistical analyses of the 20 lowest energy structures of CbpA-R1 (Table 1) were performed using the programs MolMol⁴¹ and Procheck.⁴²

Results

Description of the 3D CH₃-TOCSY Pulse Sequence. Figure 1 illustrates the 3D ¹³C-detected CH₃-TOCSY pulse sequence that was utilized to assign ¹H_{Me} and ¹³C_{Me} resonances. The pulse scheme is essentially a truncated version of the well-established HCCH-TOCSY experiment^{35,43,44} in which ¹³C detection begins immediately after FLOPSY-16⁴⁵ transfer of ¹³C magnetization between side chain carbons. The transfer pathway can be schematically described as follows:



In the first step, transverse ¹H_{Me} magnetization is created and allowed to evolve due to ¹H chemical shifts and ¹J_{CH} scalar coupling during *t*₁. A subsequent INEPT⁴⁷ step is used to transfer

(41) Koradi, R.; Billeter, M.; Wuthrich, K. *J. Mol. Graphics* **1996**, *14*, 29–32.

(42) Laskowski, R. A.; Rullmann, J. A. C.; MacArthur, M. W.; Kaptein, R.; Thornton, J. M. *J. Biomol. NMR* **1996**, *8*, 477–486.

(43) Bax, A.; Clore, G. M.; Gronenborn, A. M. *J. Magn. Reson.* **1990**, *88*, 425–431.

(44) Kay, L. E.; Xu, G. Y.; Singer, A. U.; Muhandiram, D. R.; Formankay, J. D. *J. Magn. Reson., Ser. B* **1993**, *101*, 333.

(45) Kadkhodaie, M.; Rivas, O.; Tan, M.; Mohebbi, A.; Shaka, A. J. *J. Magn. Reson.* **1991**, *91*, 437–443.

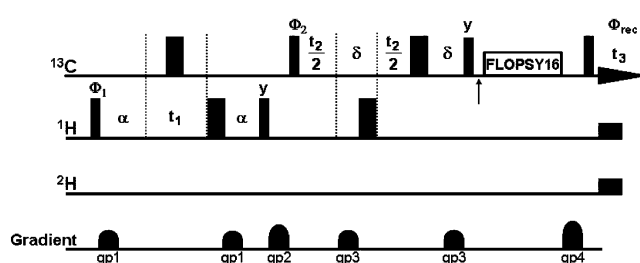


Figure 1. Pulse sequence for the ¹³C-detected CH₃-TOCSY experiment. The rf pulses on ¹H, ¹³C, and ²H were applied at 0.5, 17.0, and 4.0 ppm, respectively. The ¹³C frequency was moved to the middle of the aliphatic region (40 ppm) prior to the ¹³C–¹³C spin lock (indicated by arrow). Narrow and wide bars indicate nonselective 90 and 180° pulses, respectively. Unless indicated otherwise, all pulses were applied with phase *x*. The phase cycle is $\phi_1 = (x, -x)$, $\phi_2 = (x)$, $\phi_{\text{rec}} = (x, -x)$, and the delays were $\alpha = 1.56$ ms = $1/(4J_{\text{CH}})$ and $\delta = 475$ μs. The FLOPSY-16 mixing time was 18.8 ms using an rf field strength of 10 kHz.⁴⁶ Gradients are indicated by shapes; the gradient amplitudes were gp1 = 16%, gp2 = 17%, gp3 = 30%, and gp4 = 24%. ¹H and ²H decoupling were achieved using WALTZ-16 with 1562 kHz and 833 kHz rf fields, respectively. Quadrature detection in the indirect ¹H (*t*₁) and ¹³C (*t*₂) dimensions was achieved by the States-TPPI method applied to the phases at ϕ_1 and ϕ_2 , respectively. A recycle delay of 1.0 s was used with acquisition times of $t_{1,\text{max}} = 25.0$ ms, $t_{2,\text{max}} = 9.9$ ms, $t_{3,\text{max}} = 72.5$ ms.

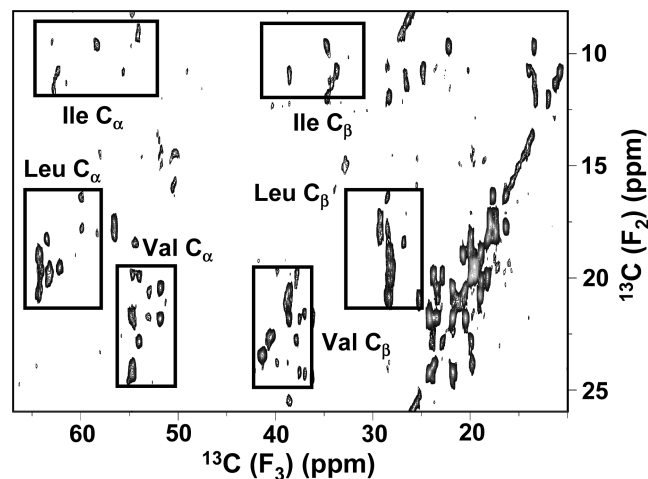


Figure 2. ¹³C (*F*₂)–¹³C (*F*₃) projection of the ¹³C-detected 3D CH₃-TOCSY experiment illustrating the correlations between ¹³C_{Me} and ¹³C_{α,β} nuclei for Val, Leu, and Ile residues.

this magnetization to the directly coupled ¹³C_{Me} spins, followed by frequency labeling of the ¹³C_{Me} chemical shifts during *t*₂. Finally, ¹³C_{Me} magnetization is transferred to other ¹³C nuclei using the FLOPSY-16 isotropic mixing scheme followed by detection of ¹³C magnetization during *t*₃ with ¹H and ²H decoupling. The ¹³C transmitter frequency is initially centered on the methyl region (~17 ppm) and is moved to the aliphatic region (~40 ppm) prior to the ¹³C–¹³C isotropic mixing period. An analogous two-dimensional experiment in which ¹³C_{Me} evolution occurs in the indirect dimension can be performed by setting *t*₁ = 0. The pulse diagram for the 2D CH₃-TOCSY experiment is included as (Supporting Information Figure 2).

CH₃-TOCSY-Based Resonance Assignment. We used the 3D ¹³C-detected CH₃-TOCSY experiment to assign ¹H_{Me} and

(46) Eletsky, A.; Moreira, O.; Kovacs, H.; Pervushin, K. *J. Biomol. NMR* **2003**, *26*, 167–179.

(47) Morris, G. A.; Freeman, R. *J. Am. Chem. Soc.* **1979**, *101*, 760–762.

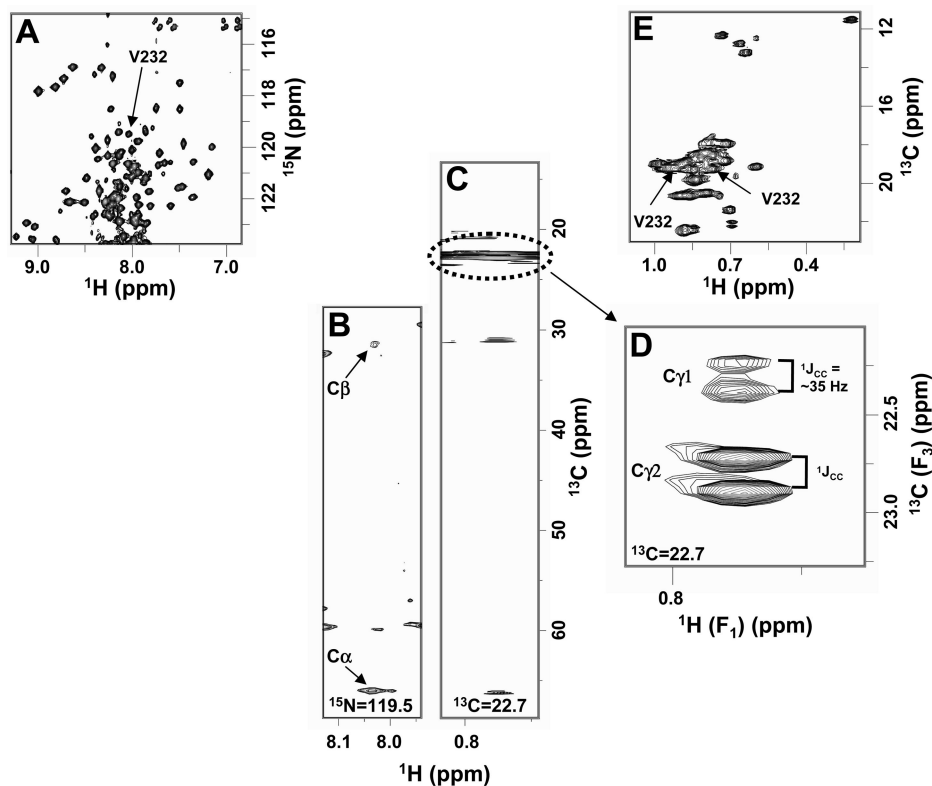


Figure 3. Establishing $^1\text{H}_\text{N}/^{15}\text{N}$ and $^1\text{H}_\text{Me}/^{13}\text{C}_\text{Me}$ correlations via $^{13}\text{C}_{\alpha,\beta}$ chemical shifts for [I, L, V]-protonated, $\text{U-}^2\text{H}/^{13}\text{C}/^{15}\text{N}$ -labeled CbpA-R1. (A) Two-dimensional $^1\text{H}-^{15}\text{N}$ TROSY spectrum; (B) ^{13}C (F_1)- $^1\text{H}_\text{N}$ (F_3) strip (^{15}N (F_2) = 119.5 ppm) for residue V232 from ^1H -detected 3D CT-HNCACB spectrum; (C) $^1\text{H}_\text{Me}$ (F_1)- ^{13}C (F_3) strip ($^{13}\text{C}_\text{Me}$ (F_2) = 22.7 ppm) from ^{13}C -detected 3D CH_3 -TOCSY spectrum; (D) expanded region of (C) showing methyl correlations; and (E) 2D $^1\text{H}_\text{Me}-^{13}\text{C}_\text{Me}$ HSQC spectrum. Resonances indicating $^{13}\text{C}_\alpha$ and $^{13}\text{C}_\beta$ correlations in the CH_3 -TOCSY spectrum are aligned with the corresponding resonances in the HNCACB spectrum, allowing sequential assignment of the complete spin system. The total measurement time for the 3D CH_3 -TOCSY spectrum was ~ 12 h.

$^{13}\text{C}_\text{Me}$ chemical shifts of 4 Ile, 5 Leu, and 7 Val residues of [I, L, V]-protonated, $^2\text{H}/^{13}\text{C}/^{15}\text{N}$ -labeled CbpA-R1. Backbone resonances were first assigned through the analysis of 3D CT-HNCACB and CT-HN(CO)CACB spectra. The 2D $^1\text{H}-^{13}\text{C}$ HSQC spectrum of [I, L, V]-protonated, $^2\text{H}/^{13}\text{C}/^{15}\text{N}$ -labeled CbpA-R1 exhibited the appropriate number of methyl resonances and, as expected, lacked resonances for other protonated side chain carbons (see Supporting Information Figure 1). The 3D ^{13}C -detected CH_3 -TOCSY spectrum, recorded in 12 h, exhibits $^1\text{H}_\text{Me}$, $^{13}\text{C}_\text{Me}$, and other side chain ^{13}C resonances of all Ile, Leu, and Val spin systems of CbpA-R1; the ^{13}C (F_2)- ^{13}C (F_3) projection is illustrated in Figure 2. Due to selective [I, L, V] protonation, limited spectral widths and high digital resolution were used in the indirect dimensions (1.2 ppm and 20 Hz/point for $^1\text{H}_\text{Me}$ (F_1) and 24 ppm and 50 Hz/point for $^{13}\text{C}_\text{Me}$ (F_2) (prior to linear prediction and zero-filling)). Sequence-specific $^1\text{H}_\text{Me}$ and $^{13}\text{C}_\text{Me}$ assignments were made by correlating $^{13}\text{C}_\alpha$ and $^{13}\text{C}_\beta$ chemical shifts that were independently linked (i) with $^1\text{H}_\text{N}/^{15}\text{N}$ chemical shifts by HNCACB and (ii) with $^1\text{H}_\text{Me}/^{13}\text{C}_\text{Me}$ chemical shifts by ^{13}C -detected CH_3 -TOCSY (Figure 3). Not all $^{13}\text{C}_\alpha$ and $^{13}\text{C}_\beta$ chemical shift pairs for Ile, Leu, and Val residues of CbpA-R1 were unique; for example, these shifts for Val 187, Val 224, and Val 252 were very similar (V187 67.14 ppm, 31.15 ppm, respectively; V224 67.10 ppm, 31.30 ppm; V252, 67.17 ppm, 31.13 ppm; Supporting Information Table 2). To break this degeneracy, we recorded a 3D CNH-NOESY⁴⁸ spectrum which allowed the methyl groups for these

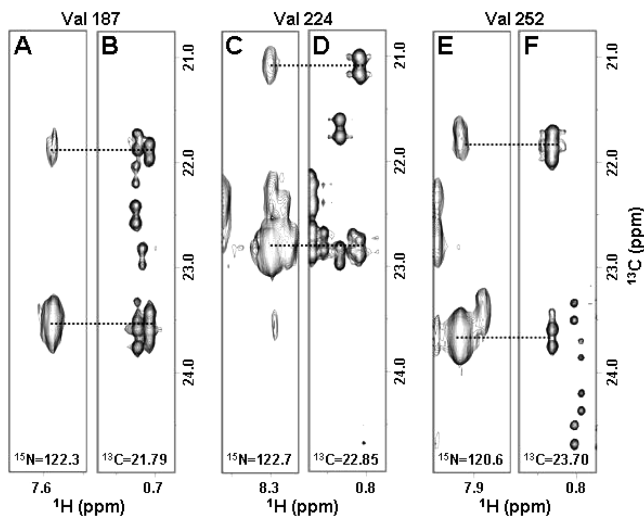


Figure 4. Breaking the degeneracy of $^{13}\text{C}_{\alpha,\beta}$ chemical shifts for sequential methyl assignments. Methyl region of (A, C, and E) ^{13}C (F_1)- ^1H (F_3) strips from the ^1H -detected 3D CNH-NOESY spectrum and (B, D, and F) $^1\text{H}_\text{Me}$ (F_1)- ^{13}C (F_3) strips from the ^{13}C -detected 3D CH_3 -TOCSY spectrum of CbpA-R1 at the ^{15}N (F_2) and $^{13}\text{C}_\text{Me}$ (F_2) chemical shifts, respectively, of Val residues 187 (A, B), 224 (C, D), and 252 (E, F). Degeneracy in the $^{13}\text{C}_\alpha$ and $^{13}\text{C}_\beta$ chemical shifts of these three Val residues required reference to data from the 3D CNH-NOESY experiment to resolve $^{13}\text{C}_\text{Me}$ resonances on the basis of their different $^1\text{H}_\text{N}$ and ^{15}N chemical shifts. The use of the 3D HNCACB, CNH-NOESY, and CH_3 -TOCSY experiments allowed complete assignment of backbone and side chain resonances for CbpA-R1 ($^1\text{H}_\text{N}$, ^{15}N , $^{13}\text{C}_{\alpha,\beta}$, etc., $^1\text{H}_\text{Me}$ and $^{13}\text{C}_\text{Me}$; see Tables 1 and 2 in Supporting Information). The total measurement time of the 3D CH_3 -TOCSY spectrum was ~ 12 h and that for 3D CNH-NOESY was 15 h.

(48) Diercks, T.; Coles, M.; Kessler, H. *J. Biomol. NMR* **1999**, *15*, 177–180.

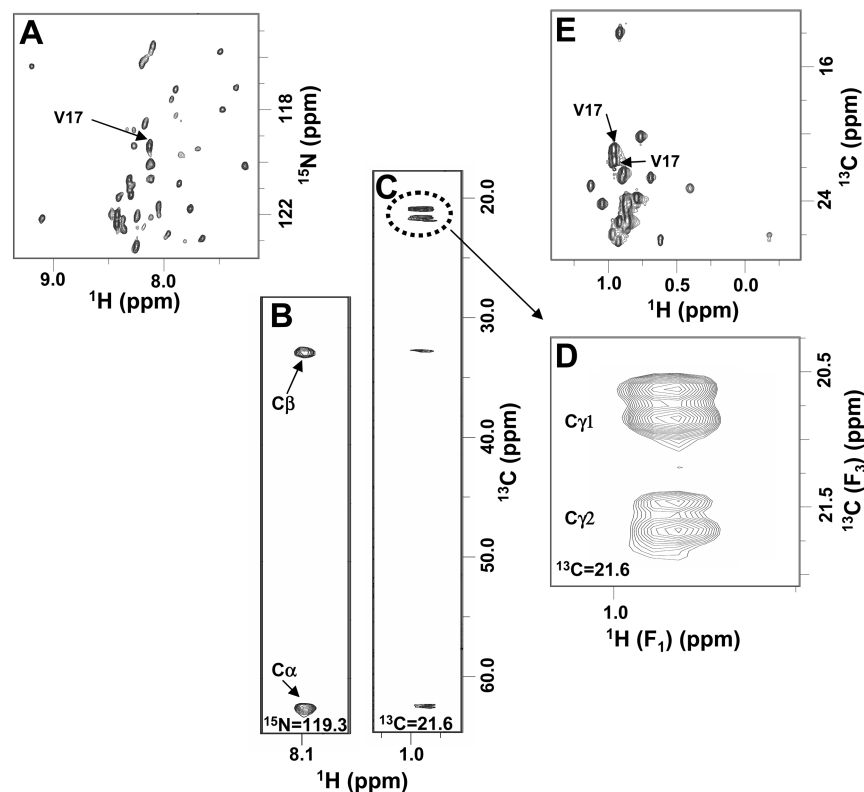


Figure 5. Establishing $^1\text{H}_\text{N}/^{15}\text{N}$ and $^1\text{H}_\text{Me}/^{13}\text{C}_\text{Me}$ correlations via $^{13}\text{C}_{\alpha,\beta}$ chemical shifts for [I, L, V]-protonated, $\text{U-}^2\text{H}/^{13}\text{C}/^{15}\text{N}$ -labeled p21-KID bound to unlabeled Cdk2. (A) Two-dimensional $^1\text{H}-^{15}\text{N}$ TROSY spectrum; (B) ^{13}C (F_1)- $^1\text{H}_\text{N}$ (F_3) strip (^{15}N (F_2) = 119.3 ppm) for residue V17 from ^1H -detected 3D HNCACB spectrum; (C) $^1\text{H}_\text{Me}$ (F_1)- ^{13}C (F_3) strip ($^{13}\text{C}_\text{Me}$ (F_2) = 21.6 ppm) from ^{13}C -detected 3D CH_3 -TOCSY spectrum; (D) expanded region of (C) showing methyl correlations; and (E) 2D $^1\text{H}_\text{Me}-^{13}\text{C}_\text{Me}$ HSQC spectrum. Resonances indicating $^{13}\text{C}_\alpha$ and $^{13}\text{C}_\beta$ correlations in the CH_3 -TOCSY spectrum are aligned with the corresponding resonances in the HNCACB spectrum, allowing sequential assignment of the complete spin system. The total measurement time for the 3D CH_3 -TOCSY spectrum was ~ 36 h for this 0.3 mM, 45 kDa complex.

three Val residues to be assigned on the basis of $^1\text{H}_\text{N}-^1\text{H}_\text{Me}$ NOE correlations (Figure 4). Importantly, due to the limited range of protonated $^{13}\text{C}_\text{Me}$ chemical shift values, the 3D CNH-NOESY spectrum was recorded with a limited spectral width in this dimension in 15 h.

We recorded a 3D ^{13}C -detected CH_3 -TOCSY spectrum for [I, L, V]-protonated, $^2\text{H}/^{13}\text{C}/^{15}\text{N}$ -labeled p21-KID (10 kDa) bound to unlabeled Cdk2 (35 kDa) to evaluate the feasibility of our $^1\text{H}_\text{Me}/^{13}\text{C}_\text{Me}$ assignment strategy in studies of a larger, more technically challenging system. For example, the solubility of this binary complex is limited to ≤ 0.3 mM in a solution comprised of 20 mM potassium phosphate and 50 mM arginine. The relatively high ionic strength of this solution significantly influences ^1H pulse lengths and sensitivity in the 800 MHz cryogenic probe but has little influence on ^{13}C pulse lengths and sensitivity.^{7,49} Analysis of the a 3D ^{13}C -detected CH_3 -TOCSY spectrum for p21-KID (recorded in 36 h) with reference to backbone and $^{13}\text{C}_\beta$ assignments made previously²³ allowed the $^1\text{H}_\text{Me}$ and $^{13}\text{C}_\text{Me}$ resonances of all 15 Ile, Leu, and Val methyl groups to be assigned. A portion of these data is illustrated in Figure 5.

Maximum Entropy Deconvolution. Evolution of $^1J_{\text{CC}}$ (~ 35 Hz for side chain $^{13}\text{C}-^{13}\text{C}$ couplings⁵⁰) during ^{13}C detection gives rise to multiplet patterns that reduce spectral resolution and signal intensity. For example, methyl carbons appear as simple doublets, while carbon atoms with couplings to two or

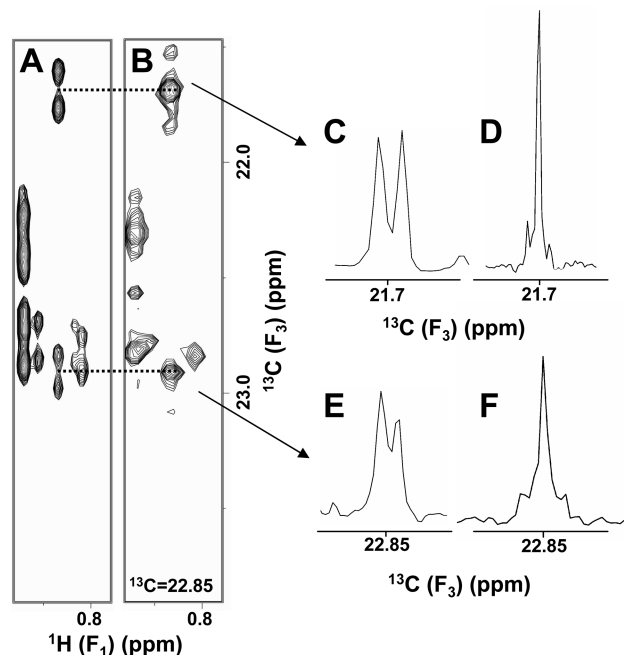


Figure 6. Maximum entropy reconstruction-deconvolution simplifies ^{13}C -detected spectra. $^1\text{H}_\text{Me}$ (F_1)- ^{13}C (F_3) strips ($^{13}\text{C}_\text{Me}$ (F_2) = 22.8 ppm) from ^{13}C -detected 3D CH_3 -TOCSY spectrum of CbpA-R1 after 3D Fourier transformation (A) and, additionally, maximum entropy reconstruction-deconvolution (B). Traces along the $^{13}\text{C}_\text{Me}$ (F_3) dimension for the two methyl resonances of V224 marked by the dotted lines in A and B are expanded in C, E and D, F, respectively. Note that methyl doublets are deconvoluted to singlets with an associated increase in S/N.

(49) Shimba, N.; Kovacs, H.; Stern, A. S.; Nomura, A. M.; Shimada, I.; Hoch, J. C.; Craik, C. S.; Dotsch, V. *J. Biomol. NMR* **2004**, *30*, 175–179.

(50) Bystrov, V. F. *Prog. Nucl. Magn. Reson. Spectrosc.* **1976**, *10*, 41–81.

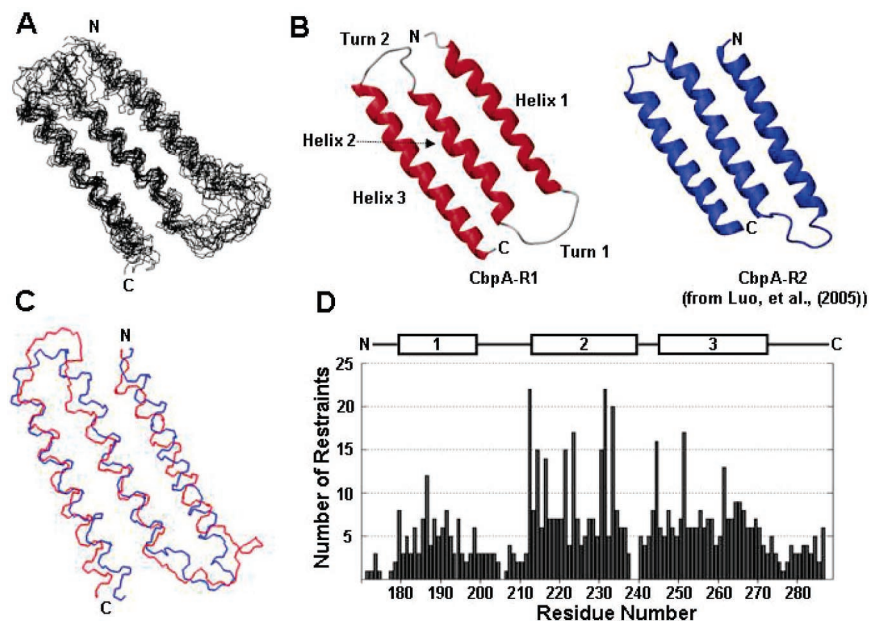


Figure 7. The structure of CbpA-R1, illustrating the limitations of using sparse restraints derived from selectively [I, L, V]-protonated proteins. (A) Superposition of 10 lowest-energy CbpA-R1 structures calculated with restraints involving only $^1\text{H}_\text{N}$ and [I, L, V] $^1\text{H}_\text{Me}$ protons using ARIA 1.2. (B) The lowest-energy structure for CbpA-R1 determined in this work (left) and for CbpA-R2 determined previously²¹ using a uniformly protonated protein sample (right). The two structures illustrated in (B) are superimposed in (C) (CbpA-R1 in red and CbpA-R2 in blue; the heavy atom backbone RMSD value is 5.03 Å). (D) The number of NOE-derived distance restraints per residue used for determination of the CbpA-R1 structure.

three magnetically nonequivalent carbon atoms exhibit more complicated multiplet patterns which hamper spectral analysis and reduce the apparent resonance intensity. Post-acquisition data processing methods, such as maximum entropy reconstruction–deconvolution (MaxEnt), can be used to partially eliminate the deleterious effects of ^{13}C – ^{13}C coupling. For example, MaxEnt processing eliminated the effects of one degree of ^{13}C – ^{13}C coupling in the CH_3 -TOCSY spectrum of CbpA-R1 (i.e., doublets were deconvoluted to singlets, triplets to doublets, etc.; Figure 6). In the case of CbpA-R1, deconvolution of ^{13}C – ^{13}C couplings was not crucial for unambiguous analysis of the 3D CH_3 -TOCSY spectrum; however, in studies of larger proteins with a larger number of Ile, Leu, and Val methyl groups and/or proteins that exhibit lower solubility and therefore lower signal intensity, MaxEnt deconvolution may be required for full spectral analysis of ^{13}C -detected data. MaxEnt spectral processing is computationally demanding and requires careful adjustment of parameters that govern how real signals and noise are differentiated. Therefore, we propose that CH_3 -TOCSY and other ^{13}C -detected spectra be processed using both conventional Fourier transformation and MaxEnt deconvolution. The two types of spectra can then be analyzed in parallel during the sequence-specific methyl group assignment process.

Global Fold of CbpA-R1 Determined Using [I, L, V]-Derived Restraints. On the basis of the backbone and Ile, Leu, and Val methyl resonance assignments for CbpA-R1 established using the methods described above, we analyzed 3D ^{13}C - and ^{15}N -edited NOESY-HSQC spectra recorded with [I, L, V]-protonated, $^2\text{H}/^{13}\text{C}/^{15}\text{N}$ -CbpA-R1 and determined $^1\text{H}_\text{N}$ – $^1\text{H}_\text{N}$, $^1\text{H}_\text{N}$ – $^1\text{H}_\text{Me}$, and $^1\text{H}_\text{Me}$ – $^1\text{H}_\text{Me}$ distance restraints (summarized in Table 1). Further, we verified amide nitrogen and proton assignments for the helical portions of CbpA-R1 through the analysis of a 4D NN-edited NOESY-HSQC spectrum. The sequence of CbpA-R1 is 78% identical to that of CbpA-R2,

whose solution structure was determined previously using conventional NMR methods.²¹ The sequences of CbpA-R1 and -R2 are highly repetitive, each containing 12 repeats of an alternative version of the leucine zipper heptad motif in which Ala frequently occurs in the “d” position instead of Leu. There are 15 Ala residues in CbpA-R1 and -R2. In addition, CbpA-R2 (CbpA-R1) contains 29 (25) and 27 (22) Lys residues. As a consequence of this unusually biased amino acid composition, analysis of 3D and 4D NOESY spectra of fully protonated, $^{13}\text{C}/^{15}\text{N}$ -labeled CbpA-R2 was complicated by the appearance of many overlapped side chain, especially methyl, resonances. Therefore, we utilized the [I, L, V] labeling strategy of Kay and co-workers in studies of CbpA-R1 to dramatically simplify the side chain resonance patterns of NMR spectra and to determine whether distance restraints derived from a subset of methyl-bearing side chains (Ile, Leu, and Val) were sufficient to accurately determine the 3D structure. The types of distance restraints obtained through this analysis are listed in Table 1. In addition to distance restraints, we utilized ψ and Φ torsion angle and H-bond restraints within the helical portions of CbpA-R1 during structure calculations.

The global fold of CbpA-R1 (Figure 7), comprised of three antiparallel α -helices in a raft-like arrangement, is similar to that of CbpA-R2 (global backbone atom RMSD of 5.03 Å; Table 1 and Figure 7). The former was based on a total of 347 NOE-derived distance restraints, while the latter was based on 2289 distance restraints.²¹ The majority of distance restraints in both cases are short or medium range (between residues i , i up to ± 4). For CbpA-R1, 16% (56) of distance restraints were long range (between residues i , $i \pm 5$, or larger), while for CbpA-R2, only 7% (149) were long range. The precision of the 20 lowest-energy structures of CbpA-R1 is best within the three α -helices (RMSD of backbone heavy atoms, 2.89 ± 0.98 Å) and poorest within the two loops between helices 1 and 2, and helices 2 and 3 (4.12 ± 0.93 Å). Helices 2 and 3 of CbpA-R1

superimpose well with those of CbpA-R2 (RMSD, 0.72 ± 0.09 and 0.93 ± 0.10 Å, respectively, and 3.35 ± 0.86 for residues 44–96); however, helix 1 of CbpA-R1 is 180° out of phase with respect to that of CbpA-R2 (RMSD, 4.46 ± 0.91 Å). On the basis of our experimental data for CbpA-R1, we cannot determine if the structural differences between CbpA-R1 and CbpA-R2 are true differences or are the consequence of inaccuracies in one or both of the solution NMR-based structures. Per residue, RMSD values for CbpA-R1 are lowest in segments with the highest concentration of methyl-bearing Ile, Leu, or Val residues (Figure 7D), suggesting that the structural differences between CbpA-R1 and CbpA-R2 in helix 1 are due to the relatively lower precision of the helix 1 structure within CbpA-R1.

Discussion

Here we have demonstrated the use of a new NMR experiment, ^{13}C -detected 3D CH_3 -TOCSY, to facilitate the assignment of protonated [I, L, V] methyl resonances of a 14 kDa protein domain, CbpA-R1. Further, we utilized this new experiment to assign protonated [I, L, V] methyl resonances of p21-KID (10 kDa) bound to Cdk2 (35 kDa). Though designed for use specifically with proteins labeled in this manner, the method offers advantages over its traditional ^1H -detected counterparts, the most obvious of which are its apparent high sensitivity and resolution. For example, in as little as 36 h, this experiment allowed complete assignment of selectively protonated methyl $^1\text{H}_{\text{Me}}$ and $^{13}\text{C}_{\text{Me}}$ resonances in a 0.3 mM, 45 kDa binary protein complex.

Other NMR experiments have been described for use in methyl group assignment, namely, ^1H -detected HMCM[CG]-CBCA¹³ and ^{13}C -detected HCC-TOCSY.¹⁴ A significant advantage of the CH_3 -TOCSY (presented here) is the ability to efficiently achieve high resolution in all dimensions. Using only the ^1H -detected out-and-back experiments, Tugarinov et al. were able to assign 95 and 93% of Ile and Val residues, respectively.¹³ However, poor resolution (~ 97 Hz/pt in the indirect aliphatic ^{13}C ($^{13}\text{C}_{\text{aliphatic}}$) dimension) and chemical shift degeneracy precluded full assignment of Leu residues ($\sim 64\%$ were assigned) using these methods alone.¹³ The ^{13}C -detected CH_3 -TOCSY experiment, which affords optimal digital resolution in all dimensions (especially the directly detected $^{13}\text{C}_{\text{aliphatic}}$ dimension spanning almost 70 ppm, where resolution of 5 Hz/pt was achieved), is an alternative approach that can overcome digital resolution limitations. The use of narrow spectral widths allows optimal digitization of the indirect dimensions using relatively small numbers of data points while the large spectral width of the directly detected $^{13}\text{C}_{\text{aliphatic}}$ dimension can be extensively digitized without significantly extending the overall acquisition time. This latter benefit improves the precision with which side chain carbon chemical shifts can be determined which, in turn, influences the extent to which $^1\text{H}_{\text{Me}}/^{13}\text{C}_{\text{Me}}$ chemical shifts can be unambiguously assigned to specific residues. Attempts to gain similar resolution in the $^{13}\text{C}_{\text{aliphatic}}$ dimension using the ^1H -detected HMCM[CG]CBCA experiment would result in experiment times in excess of 100 hours (using upward of 300 complex points in the indirect $^{13}\text{C}_{\text{aliphatic}}$ dimension). In addition, while the “out-and-back” method is designed for use with “linearized” spin systems, the CH_3 -TOCSY experiment is suitable with both (linearized and nonlinearized) variants. While both of these experiments make

use of the abundant ^1H magnetization of selectively protonated methyl residues, the CH_3 -TOCSY, due to its reliance on isotropic mixing for ^{13}C magnetization transfer, may be less subject to signal loss due to the generation of multiple quantum spin terms as is observed with the COSY-type transfer steps of the HMCM[CG]CBCA experiment.¹³ This advantage may in part counteract the inherent disadvantage associated with directly detecting lower γ ^{13}C nuclei. In addition, in the case of p21/Cdk2, the use of few ^1H pulses and ^{13}C detection minimizes radio frequency losses due to the relatively high ionic strength of this solution.

The CH_3 -TOCSY experiment (presented here) and the HCC-TOCSY¹⁴ experiment have been demonstrated using significantly different isotope-labeled protein samples. We have used selectively [I, L, V] methyl-protonated, uniformly $^2\text{H}/^{13}\text{C}/^{15}\text{N}$ -labeled proteins, while Pervushin and co-workers used either fully or 10% protonated, uniformly $^{13}\text{C}/^{15}\text{N}$ -labeled samples. In addition, the manner in which ^1H and ^{13}C chemical shift evolution is achieved in the two experiments is different. Our CH_3 -TOCSY experiment utilizes independent, sequential evolution of ^1H and ^{13}C single quantum coherence during t_1 and t_2 , respectively, with INEPT⁴⁷ transfer from $^1\text{H}_{\text{Me}}$ to $^{13}\text{C}_{\text{Me}}$ prior to FLOPSY isotropic mixing.⁴⁵ In contrast, the HCC-TOCSY experiment uses constant-time evolution of heteronuclear, multiple quantum coherence with systematic movement of either ^1H or ^{13}C 180 pulses, respectively, to achieve ^1H and ^{13}C chemical shift evolution.¹⁴ In the IP-HCC-TOCSY version of the experiment, the constant-time period is ~ 28 ms in total to allow refocusing of $^1J_{\text{CC}}$ coupling. At the same time, this long delay allows significant relaxation of magnetization terms that ultimately give rise to detected ^{13}C magnetization. In the SE-HCC-TOCSY version of the experiment, the constant-time delay is reduced to minimize relaxation although this compromises the pure-phase character of the detected ^{13}C magnetization after FLOPSY isotropic mixing. With regard to selectively [I, L, V] methyl-protonated, uniformly $^2\text{H}/^{13}\text{C}/^{15}\text{N}$ -labeled proteins, our CH_3 -TOCSY experiment and either the IP or SE versions of the HCC-TOCSY experiment will give very similar 3D spectra exhibiting essentially identical $^1\text{H}_{\text{Me}}/^{13}\text{C}_{\text{Me}}$ to side chain ^{13}C correlations. However, we have noticed that our CH_3 -TOCSY experiment yields 3D spectra with high S/N with relatively short acquisition times in comparison with the HCC-TOCSY experiment. For example, we recorded the 3D spectrum of 1 mM CbpA-R1 illustrated in Figure 2 in 12 h, while Pervushin and co-workers recorded a 3D IP-HCC-TOCSY spectrum for 1 mM Ccm-E, which exhibits the types of correlations exhibited in our 3D spectrum plus many others, in 117 hours.¹⁴

Carbon-detected methods, however, are not without disadvantages. The most obvious disadvantage is the low sensitivity associated with detection of ^{13}C nuclei (the magnetogyric ratio, γ , of ^{13}C is approximately one-fourth that of ^1H , decreasing sensitivity by about a factor of 8). This shortcoming, however, is mitigated by the utilization of abundant methyl ^1H magnetization, highly sensitive cryogenic probes optimized for ^{13}C and ^1H detection, and shorter pulse programs. Additional complications accompany the use of ^{13}C -detected experiments in the form of ^{13}C – ^{13}C scalar couplings. Due to high resolution in the direct dimension, ~ 35 – 55 Hz $^1J_{\text{CC}}$ couplings are resolved, causing side chain carbons to be detected as multiplets. Several methods have been proposed to alleviate this problem, including multiple-

band-selective ^{13}C -decoupling during acquisition,⁵¹ spin-state selection through IPAP-type acquisition,^{46,52} constant-time ^{13}C evolution,⁵¹ and maximum entropy reconstruction–deconvolution method,^{49,53} as used here. Each of the former methods results in a decreased signal-to-noise ratios (S/N) and, in the case of IPAP acquisition, longer experiment times and additional delays that may be detrimental in the study of large systems with short T_2 relaxation times. Here, we show that postacquisition data processing by maximum entropy reconstruction–deconvolution combined with standard FT-based methods is an effective means of simplifying the analysis of ^{13}C -detected spectra. This method, in addition to allowing the use of shorter experiment times, introduces no additional delays and does not require implementation of complicated multiple-band decoupling schemes. The performance of MaxEnt in current implementations, however, is limited by its ability to deconvolve only one order of coupling and, thus, exhibits significant improvement of the spectra only in peaks with one coupling pattern. In principle, the kernel function could be adjusted to manifest triplets rather than doublets on a frequency-selective basis. However, deconvolution of a doublet and a triplet simultaneously in the same frequency domain spectrum is not currently feasible. Thus, the deconvolution algorithm, as presented here, is most useful in simplifying the methyl region of a 3D CH_3 -TOCSY spectrum.

It was observed that the most significant drawback to resonance assignment by the present strategy is likely to involve the extensive chemical shift degeneracy that would be expected when applying this method to larger proteins with high [I, L, V] content. Nevertheless, the use of ^{13}C -detected experiments to be developed in the future will establish correlations between $^1\text{H}_\text{N}$, ^{15}N , or $^{13}\text{C}'$ chemical shifts and $^{13}\text{C}_\gamma$, in addition to $^{13}\text{C}_{\alpha,\beta}$, chemical shifts and will likely help to assuage this problem and reduce the ambiguity of resonance assignments in larger proteins.

In determining the global fold of CbpA-R1, we utilized the methyl protonation strategy to obtain $^1\text{H}_\text{Me}$ and $^{13}\text{C}_\text{Me}$ chemical shifts of Ile, Leu, and Val residues. This approach would not normally be required for a protein of this size (~14 kDa). However, the repetitive sequence characteristics and extensive helical structure of this protein resulted in highly degenerate NMR spectra. Thus, the use of the methods presented here facilitated resonance assignment and structure determination and are likely to be applicable to other proteins exhibiting similar complications. In addition, we have demonstrated the application of these methods to a larger protein complex (~45 kDa), which suggests its utility in studies of biomolecules much larger than 14 kDa. Shortcomings, however, lie in the quality of the protein structures determined by this method. Although we and others¹⁰ have demonstrated that valuable information can be obtained from the use of low resolution global folds, we concede that the use of a limited number of distance restraints results in structures characterized by lower precision and accuracy as compared with those determined using conventional approaches with fully protonated $^{13}\text{C}/^{15}\text{N}$ proteins. It is clear, however, that improvements to structures determined in this manner can be

achieved through the use of additional restraint information, such as residual dipolar couplings (RDCs). It has been demonstrated that $^1\text{H}-^{15}\text{N}$, $^{13}\text{C}_\alpha-^{13}\text{C}'$, $^{15}\text{N}-^{13}\text{C}'$, two-bond $^1\text{H}_\text{N}-^{13}\text{C}'$, and three-bond $^1\text{H}_\text{N}-^{13}\text{C}'$ dipolar couplings can be used to orient discrete peptide planes in polypeptide structures determined with low densities of NOEs.⁵⁴ In this case, refinement against these RDC restraints resulted in a significant increase in the precision of the structures, with global RMSD values decreasing from 5.5 to 2.2 Å.⁵⁴ If this approach was taken to measure backbone RDCs and enhance structure quality, the CH_3 -TOCSY could also be used to derive aliphatic $^{13}\text{C}-^{13}\text{C}$ RDC values (from directly detected side chain $^{13}\text{C}-^{13}\text{C}$ couplings), which could then be used to further improve structure quality. This approach was recently presented by Vögeli et al., in which a 2D $^{13}\text{C}-^{13}\text{C}$ TOCSY experiment was used to measure $^{13}\text{C}_\text{Me}$ dipolar couplings before and after weak alignment in Pf1 phage.⁵⁵

While advances in hardware serve to push the boundaries of protein structure determination by NMR, it is quite clear that the selective [I, L, V] methyl protonation strategy of Kay and co-workers will be required when studying the structure of proteins and protein assemblies of sizes greater than ~40 kDa. In these cases, the ^{13}C detection-based method described here, and others to be developed in the future, may prove to be advantageous for establishing sequence-specific methyl resonance assignments. In addition, the increased availability of cryogenic probes capable of both ^{13}C and ^1H detection will likely make the applications presented here widely applicable to the NMR community.

In addition to providing a facile route to resonance assignments and global fold determination, these methods present other possibilities in applications, such as mapping intermolecular interactions by NMR. For cases of proteins with unknown structure but for which a reasonable homology model exists, the sensitivity and spectral simplification of these methods provide a fast and effective route to Ile, Leu, and Val methyl resonance assignments, allowing the site(s) of small-molecule or macromolecular interactions to be identified.

Conclusions

In summary, complete resonance assignments of Ile, Leu, and Val methyl groups have been made in two selectively [I, L, V] methyl-protonated, uniformly $^2\text{H}/^{13}\text{C}/^{15}\text{N}$ -labeled proteins. The first, CbpA-R1, is a 119 residue domain from a bacterial surface protein that exhibits a highly repetitive sequence, extensively helical secondary structure, and yields highly complex NMR spectra. The second protein sample, a complex of isotope-labeled p21-KID and unlabeled Cdk2, is roughly 45 kDa in size and of limited solubility (~0.3 mM) and stability. To achieve these assignments, we used standard ^1H -detected NMR methods in addition to a new ^{13}C -detected CH_3 -TOCSY pulse sequence which utilizes abundant ^1H methyl magnetization that is ultimately transferred to and detected at all aliphatic side chain carbon sites. The latter method, in combination with conventional backbone resonance assignment methods as illustrated here, allows $^1\text{H}_\text{Me}/^{13}\text{C}_\text{Me}$ chemical shifts to be determined with high resolution in an efficient manner and for these to be correlated with the chemical shift values of other side chain

(51) Vogeli, B.; Kovacs, H.; Pervushin, K. *J. Biomol. NMR* **2005**, *31*, 1–9.
(52) Bermel, W.; Bertini, I.; Duma, L.; Felli, I. C.; Emsley, L.; Pierattelli, R.; Vasos, P. R. *Angew. Chem., Int. Ed.* **2005**, *44*, 3089–3092.
(53) Shimba, N.; Stern, A. S.; Craik, C. S.; Hoch, J. C.; Dotsch, V. *J. Am. Chem. Soc.* **2003**, *125*, 2382–2383.

(54) Mueller, G. A.; Choy, W. Y.; Yang, D.; Forman-Kay, J. D.; Venters, R. A.; Kay, L. E. *J. Mol. Biol.* **2000**, *300*, 197–212.
(55) Vogeli, B.; Kovacs, H.; Pervushin, K. *J. Am. Chem. Soc.* **2004**, *126*, 2414–2420.

carbons. Side chain $^{13}\text{C}_{\alpha,\beta}$ chemical shifts, for example, can then be related to $^1\text{H}_\text{N}/^{15}\text{N}$ backbone chemical shifts by reference to data from the 3D HNCACB experiment, allowing sequence-specific assignment of the [I, L, V] methyl resonances. The ^{13}C -detected CH_3 -TOCSY experiment provides a new avenue to these methyl assignments and may present advantages over ^1H detected methods under certain circumstances. As the selective [I, L, V] labeling strategy is applied to more and larger protein systems, NMR methods based on ^{13}C detection, such as that illustrated here, should be routinely applied as a complement to ^1H -detected methods. In fact, ^{13}C detection-based methods may be the most efficient route to correlate methyl resonances with other aliphatic carbon resonances in cases where ^1H detection is suboptimal, for example, with high ionic strength, low concentration protein solutions.⁴⁹ ^{13}C detection-based methods, in combination with selective methyl protonation, will contribute significantly in further extending the size limit that governs structure determination and dynamic analysis of proteins in solution using NMR spectroscopy.

Acknowledgment. The authors acknowledge Dr. Steve Unger (Accelrys) for assistance with software modifications related

to Felix and Rowland NMR Toolkit compatibility, and Dr. Bradley Dickerson for helpful discussion. This work was supported by the American Lebanese Syrian Associated Charities (ALSAC) and NIH through a Cancer Center CORE grant (P30 CA21765; St. Jude Children's Research Hospital) and R01 CA82491 (R.W.K.). Financial support from the National Institutes of Health for the development of the Rowland NMR Toolkit, via grants GM047467 (Gerhard Wagner, PI) and RR-020125 (Jeffrey Hoch, PI) is gratefully acknowledged.

Supporting Information Available: One figure showing a ^1H - ^{13}C HSQC spectrum of selectively protonated CbpA-R1 demonstrating the degree of isotopic labeling, one figure describing a two-dimensional version of the three-dimensional experiment submitted herein, a table of backbone chemical shift values for CbpA-R1, and a table of side chain chemical shift values for selectively protonated residues. Also available are complete refs 21 and 39. This material is available free of charge via the Internet at <http://pubs.acs.org>.

JA058587A